Developing CALPHAD databases for thermophysical properties of metals and alloys

Hai-Lin Chen, Masoomeh Ghasemi, Qing Chen*

Thermo-Calc Software AB

Phase diagrams are the beginning of wisdom

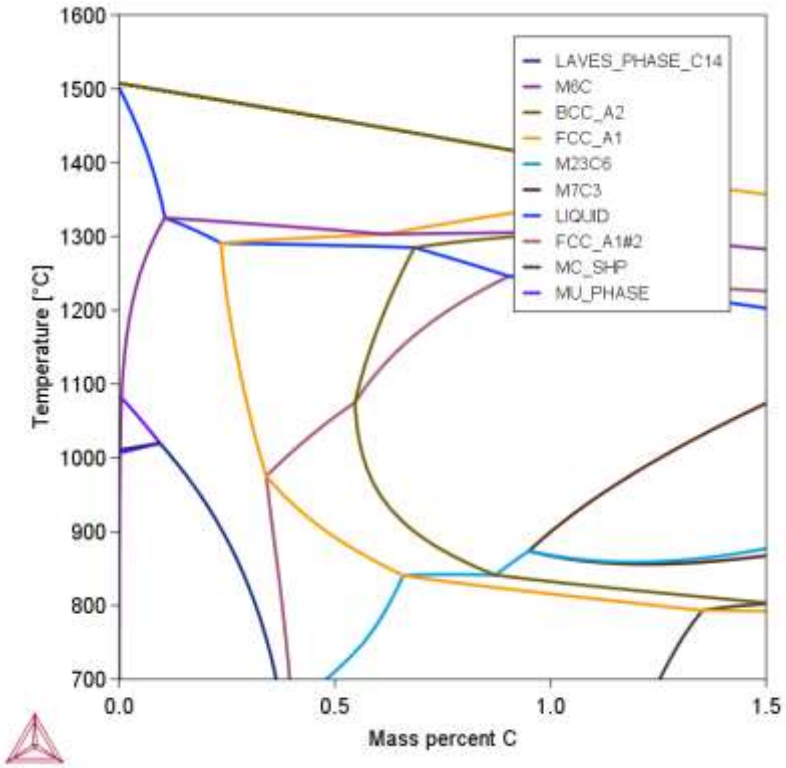

Phase diagram for a M42 high speed steel, Fe-4Cr-5Mo-8W-2V-0.3Mn-0.3Si-C(wt%).

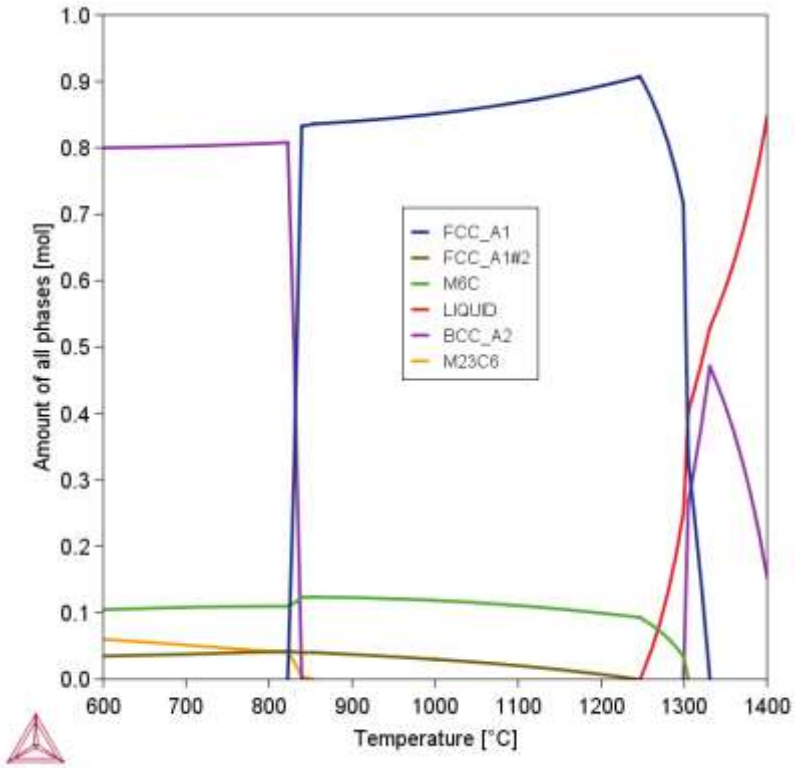

Property diagram for a M42 high speed steel, Fe-4Cr- 5Mo-8W-2V-0.3Mn-0.3Si-0.9C.

We need an Einstein in metallurgy to be able to see into 5 or 6 dimensional space – and some genius – and he would have to be a very great one, to predict what phase constitution in such systems would be, if the fearful amount of the currently necessary experimental work is to be avoided.

- Robert F. Mehl, 1959

- Collected experimental and computational data are used to fit functions.
- Functions are used to calculate phase equilibria, including phase diagrams.

Experimental phase diagram and thermochemical data → Determine Gibbs energy functions for each phase: $G = f(x,T,P)$ → Calculated phase diagram → Combine binaries and ternaries to predict multi-component systems

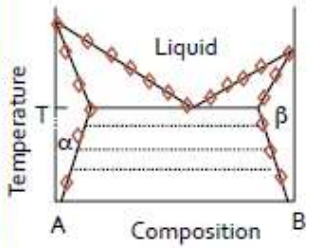

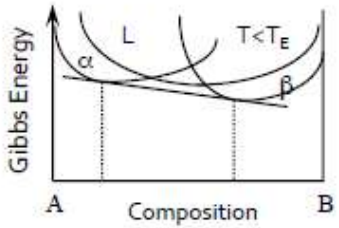

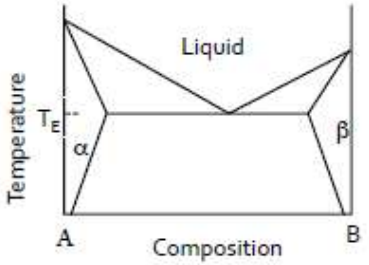

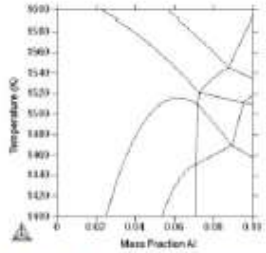

Al isopleth for 8 component system

$$G^{\phi} = G^{0} + G^{ideal} + G^{excess}$$

Binaries → Ternaries → Quaternaries → n^{th} Order Systems

➡ True quaternary compounds are rare in metallic systems

➡ Assessment of ternary systems is usually sufficient for the description of a multicomponent system

➡ Same methodology can be applied to the description of other property data

From Dr. C. Campbell, NIST, USA

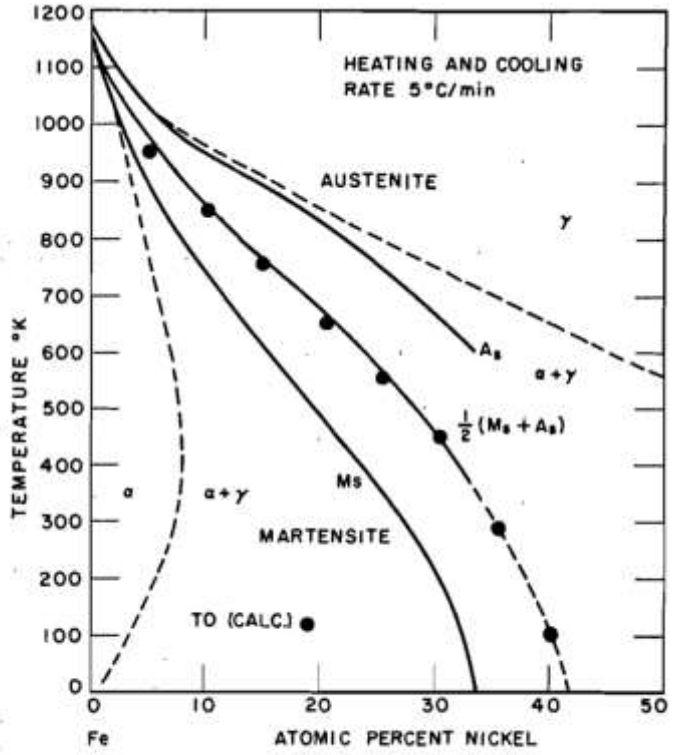

Fig. 1—The M_s-A_s diagram, determined by resistance measurements. The dashed lines are the $\alpha/\alpha+\gamma$ and $\alpha+\gamma/\gamma$ phase boundaries of the equilibrium diagram.

by Larry Kaufman and Morris Cohen

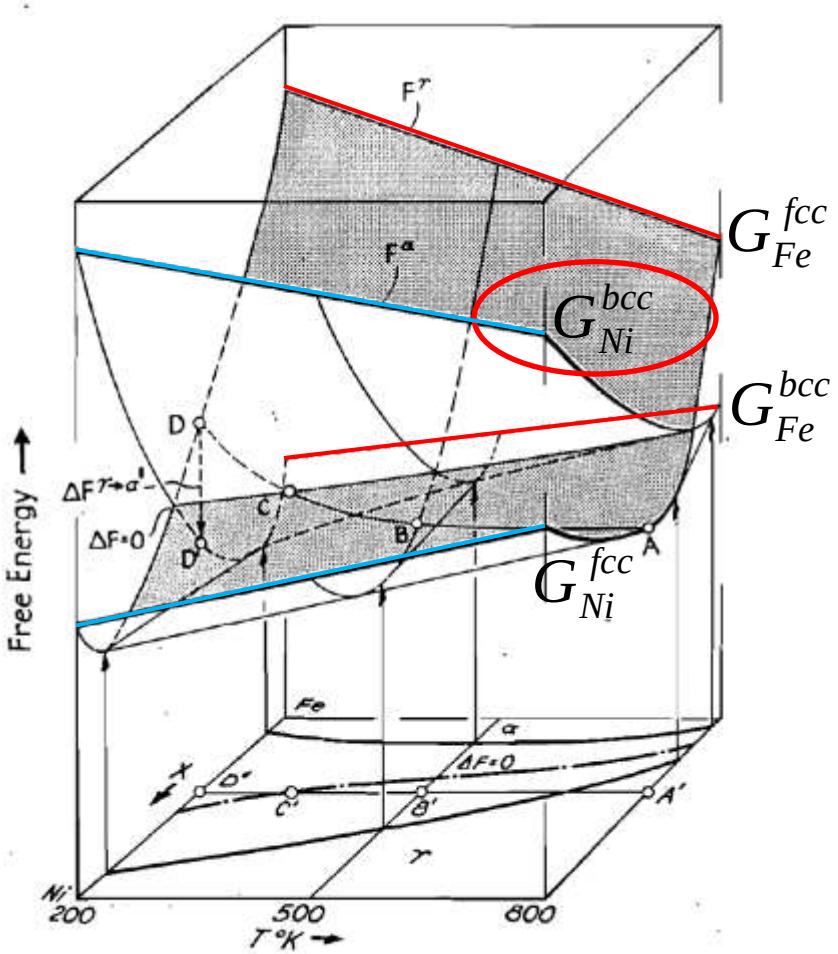

Fig. 6—Schematic representation of F^γ and F^α surfaces as a function of x and T.

TRANSACTIONS AIME

OCTOBER 1956, JOURNAL OF METALS—1393

$$G_m^{\alpha} = \sum_i x_i^{\alpha} {}^{o}G_i^{\alpha} - TS_m^{ideal\alpha} + {}^{E}G_m^{\alpha}$$

$${}^{E}G_m^{\alpha} = \sum_{i \neq j} x_i x_j L_{i,j}^{\alpha}$$

$$+ \sum_{i \neq j \neq k} x_i x_j x_k L_{i,j,k}^{\alpha}$$

$$+ \sum_{i \neq j \neq k \neq l} x_i x_j x_k x_l L_{i,j,k,l}^{\alpha}$$

$$+ \cdots$$

$$\prod_{i=2}^{n} x_i$$

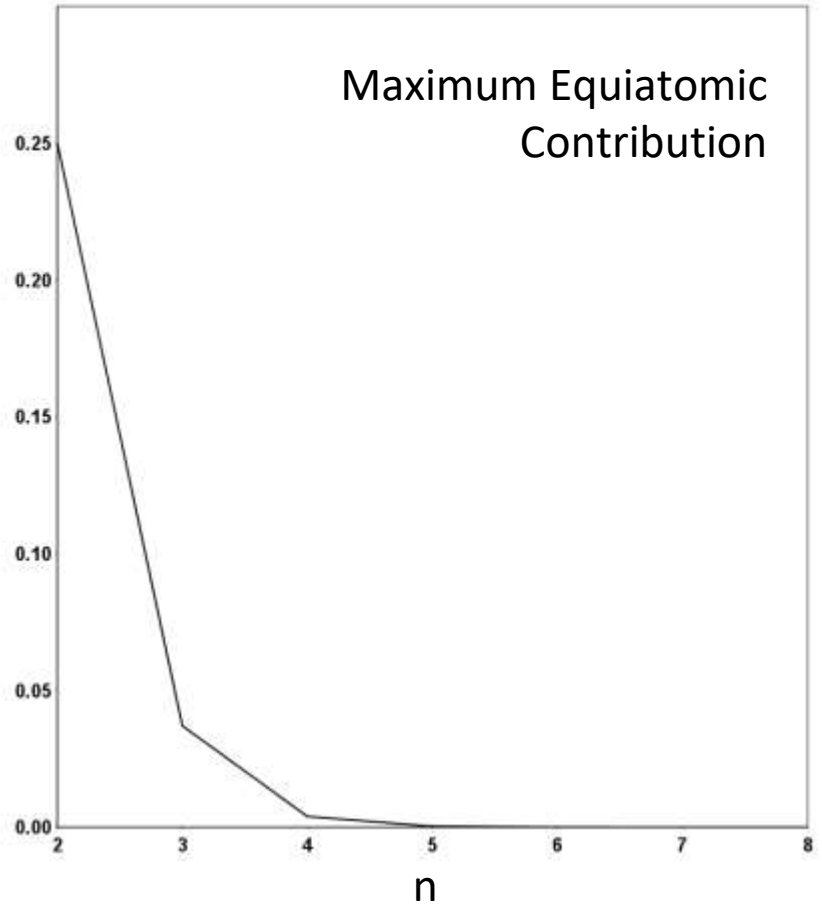

Atomic mobility Database

$$M_i = \frac{1}{RT} D_0 \exp\left(\frac{-Q_i}{RT}\right)$$

$$\Phi_i = RT \ln\left(RTM_i\right)$$
$$= -Q_i + RT \ln D_0$$

$$\Phi_i = \sum_j x_j \Phi_i^j + {}^E\Phi_i$$

$${}^E\Phi_i = \sum_j \sum_{k>j} x_j x_k \left[\sum_{\nu=0} {}^\nu\Phi_i^{jk} \left(x_j - x_k\right)^\nu + \sum_{l>k} x_l \left(\Phi_i^{jkl} + \cdots\right) \right]$$

$$M_i = \exp\left(\frac{\Phi_i}{RT}\right)\frac{1}{RT}$$

$$[M) = \begin{pmatrix} M_1 \\ M_2 \\ \bullet \\ M_{10} \end{pmatrix}$$

Chemical Diffusivity

$$[D] = \begin{bmatrix} D_{11} & D_{12} & \bullet & D_{19} \\ \bullet & \bullet & & \\ \bullet & & \bullet & \\ D_{91} & & & D_{99} \end{bmatrix}$$

Self-diffusivity
Impurity diffusivity
Intrinsic diffusivity
Tracer diffusivity

Redlich-Kister Expansion (RKE)

J.O. Andersson and J. Ågren, J. Appl. Phys., 72 (1992) 1350.

lattice parameter	molar volume	density	thermal expansion coefficient	relative length change	lattice mismatch

$$V_m(T) = V_0 \exp\left(\int_{T_0}^{T} 3\alpha dT\right)$$

$$= V_0 \exp(V_A)$$

$$V_0 = \sum_i x_i V_0^i + {}^E V_0$$

$$V_A = \sum_i x_i V_A^i + {}^E V_A$$

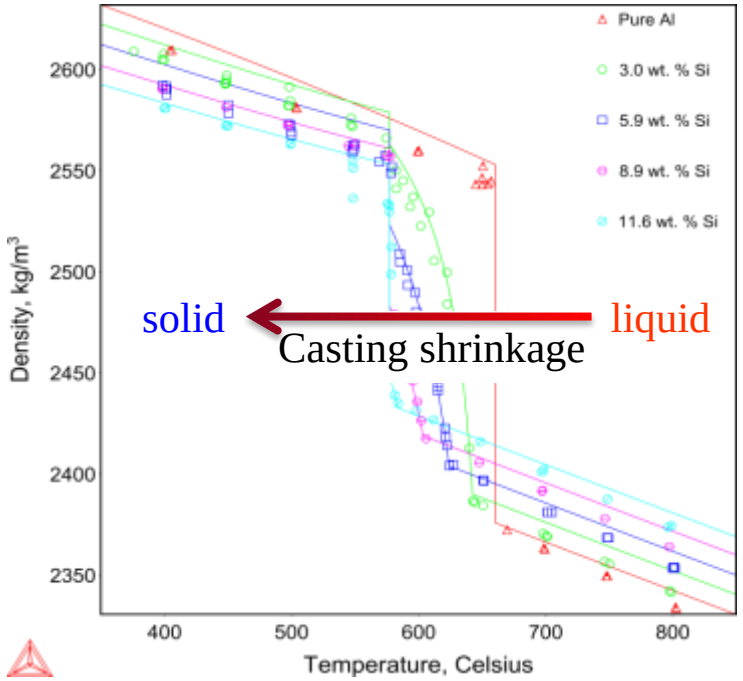

The effect of Si content on the densities of Al-Si alloys

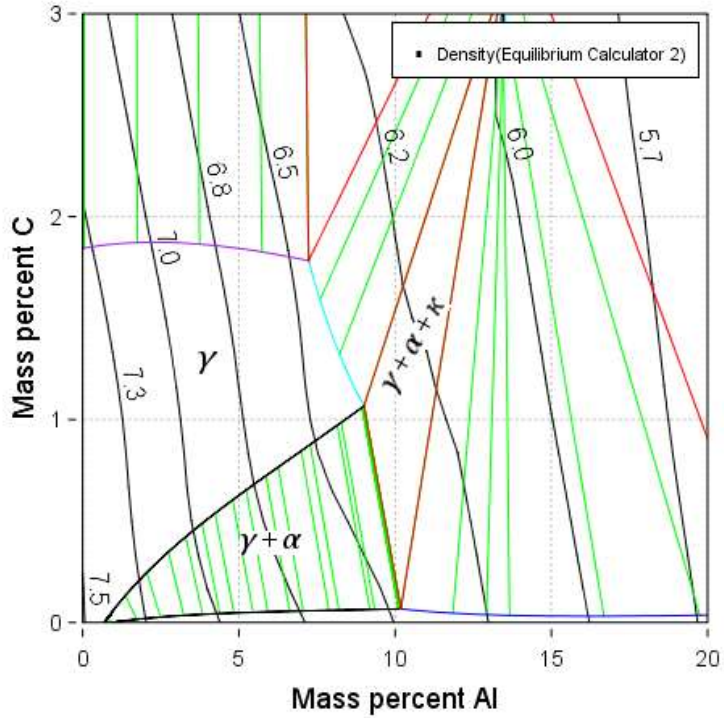

Al-Fe-C phase diagram and iso-density contour lines at 1100 °C, calculated with TCFE9. (g/cm3)

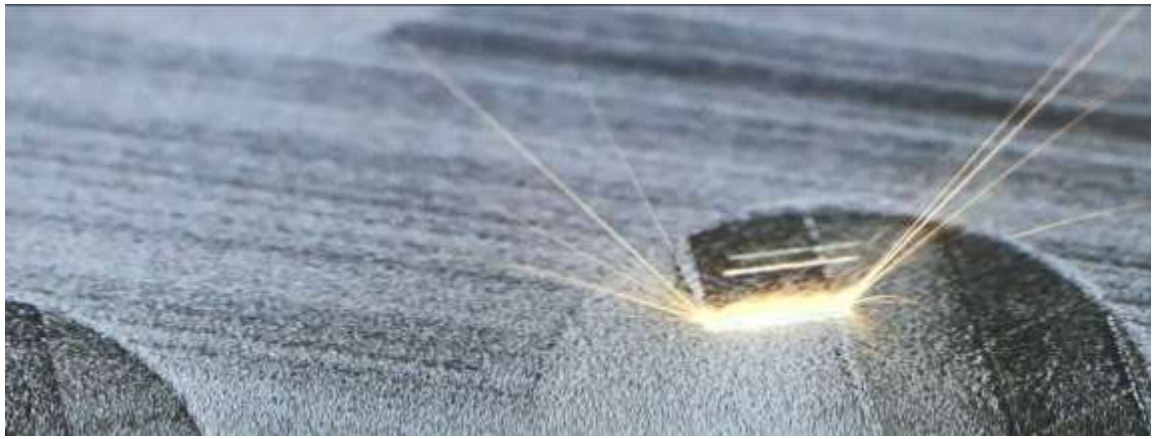

https://new.siemens.com/global/en/company/stories/research-technologies/additivemanufacturing/additive-manufacturing-simulation-of-molten-metal.html

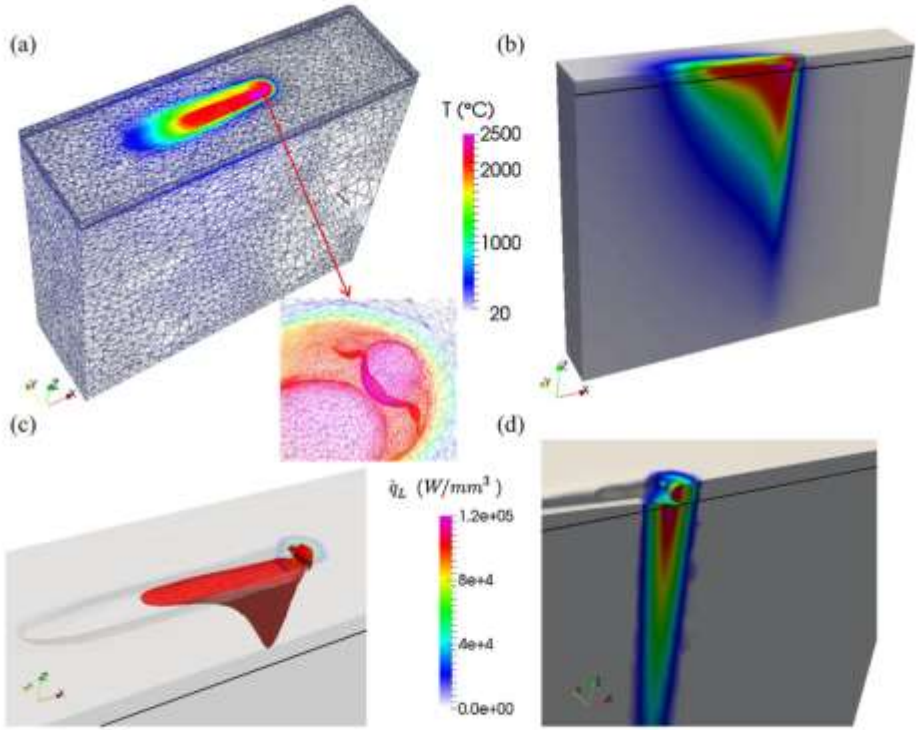

Fig. 7. Snapshot for reference case at $t = 2$ ms illustrating (a) the FE mesh adaptation in the vicinity of the pool surface and (a, b) temperature field (cut view along the vertical symmetry plane), (c) the melt pool defined by regions of temperature higher or equal to the melting temperature in the material domain (transparent rendering is active in order to show the whole melt pool), and (c, d) position of the heat source and distribution of the volumetric heat source term (cut view along the vertical symmetry plane). Gas is removed and the black line shows the powder/substrate boundary.

Table 1
Material properties for pure alumina.

Properties	Symbol	Value	Unit	Reference
Solid, liquid, gas	s, l, g			
Powder zone	Z_1	s, g		
Dense matter zone	Z_2	s, l		
Volume fraction of phase ϕ_j in zone Z_i	$g_{Z_i}^{\phi_j}$			
Volume fraction of zone Z_i in material domain D_1	$g_{D_1}^{Z_i}$			
Solid and liquid alumina density	ρ^s, ρ^l	3800	$kg\,m^{-3}$	[37]
Gas density	ρ^g	1.3	$kg\,m^{-3}$	
Enthalpy per unit mass of material domain (D_1)	$\langle h \rangle^{D_1}$	Fig. 5(a)	$J\,kg^{-1}$	[25]
Heat capacity of gas	C_p^g	1000	$J\,kg^{-1}\,K^{-1}$	
Alumina conductivity	λ^a	Eq. (28)	$W\,m^{-1}\,K^{-1}$	[38]
Gas conductivity	λ^g	0.024	$W\,m^{-1}\,K^{-1}$	
Conductivity of zone i	$\langle \lambda \rangle^{Z_i}$	Fig. 5(b)	$W\,m^{-1}\,K^{-1}$	[39]
Viscosity of liquid alumina	μ^l	0.069	$Pa\,s$	[40]
Viscosity of gas	μ^g	0.000024	$Pa\,s$	
Viscosity of zone i	$\langle \mu \rangle^{Z_i}$	Fig. 5(c)	$Pa\,s$	
Surface tension liquid/gas	γ	0.67	$N\,m^{-1}$	[41]

Thermal conductivity / resistivity

Electric conductivity / resistivity

Viscosity

Their temperature dependence

Their composition dependence

Thermal conductivity

$$\boldsymbol{k = k_e + k_g}$$

Wiedemann-Franz law

$$\frac{\kappa_e}{\sigma} = L_0 T$$

The Sommerfeld value of the Lorenz number

$$L_0 = \frac{\pi^2}{3} \cdot \frac{k_B^2}{e^2} = 2.4453 \times 10^{-8} W \cdot \Omega / K^2$$

Major scatterings

Electrical resistivity & Electronic thermal conductivity

- Electron-phonon scattering
- Electron-electron scattering
- Impurity scattering
- Defect scattering

Lattice thermal conductivity

- Phonon-electron scattering
  - low temperatures
- Phonon-Phonon scattering
  - Umklapp processes high temperatures
- Phonon-Phonon scattering
  - Normal processes
- Impurity and defect scatterings

Au-Cu, electrical resistivity

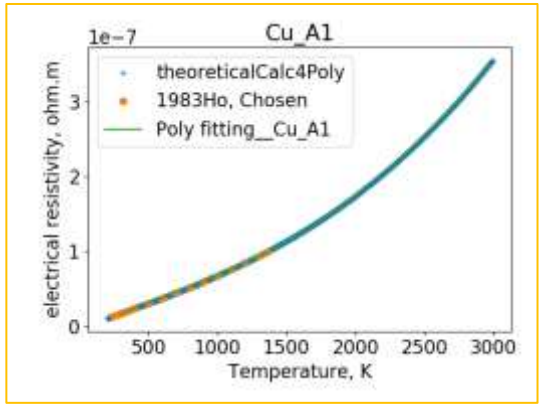

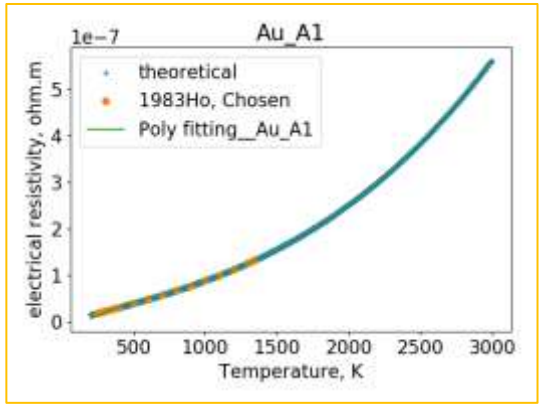

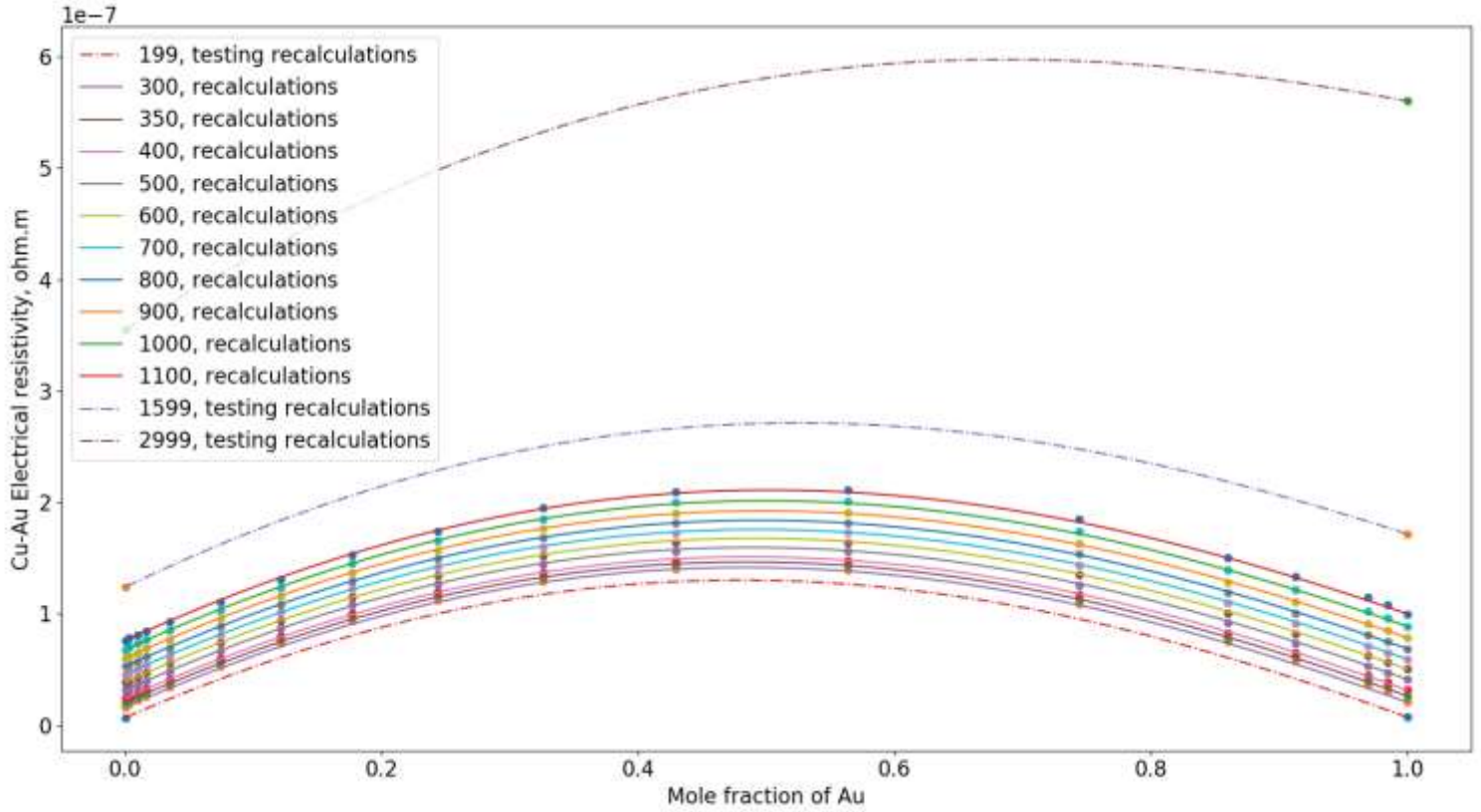

Au-Cu, thermal conductivity

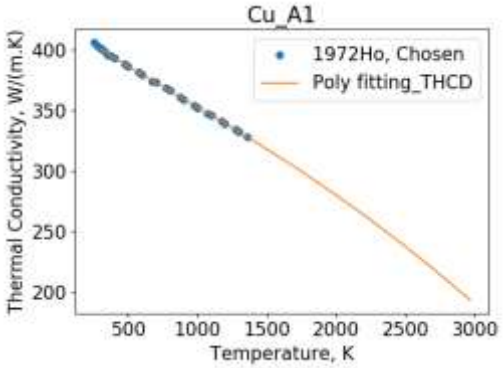

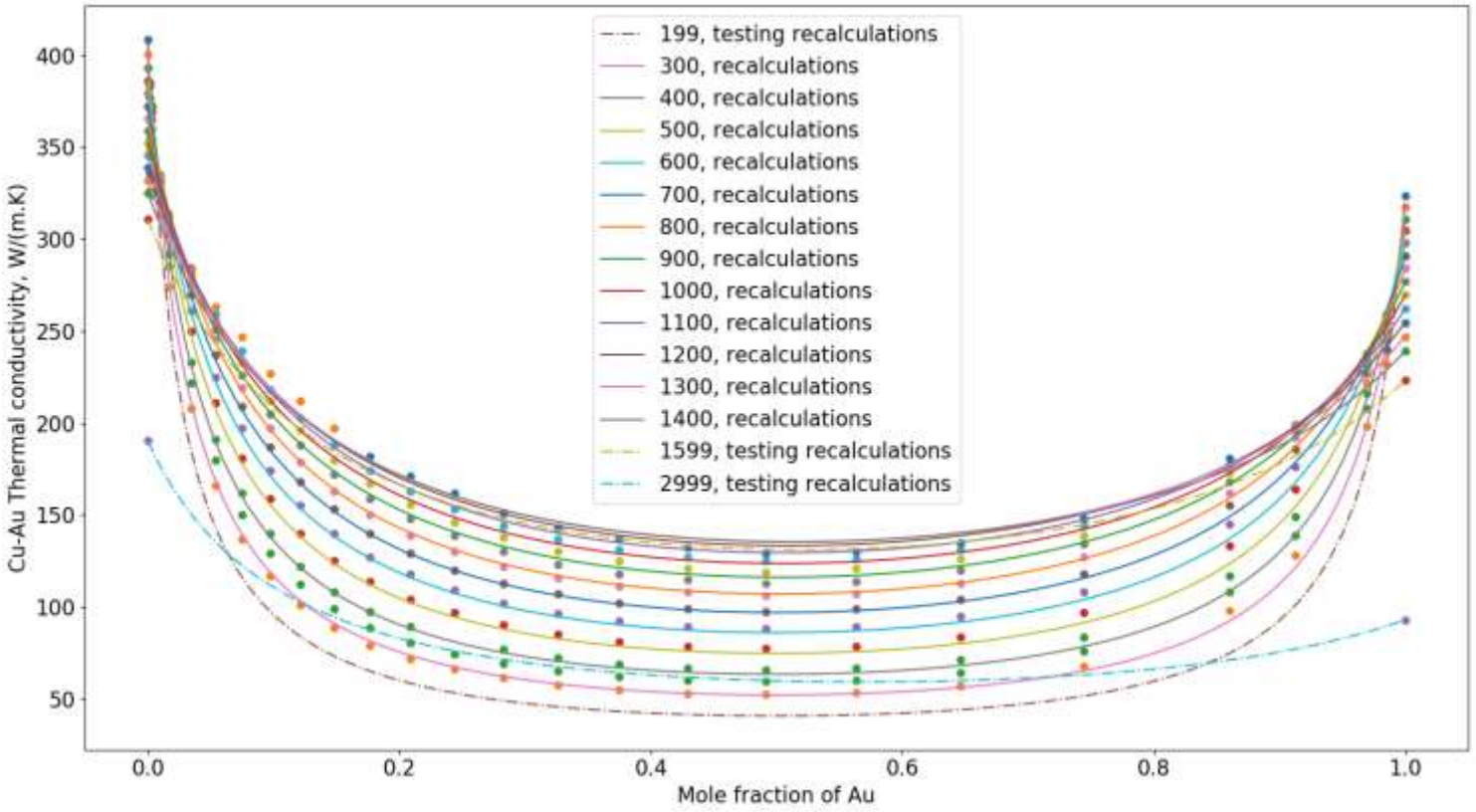

HEA alloys

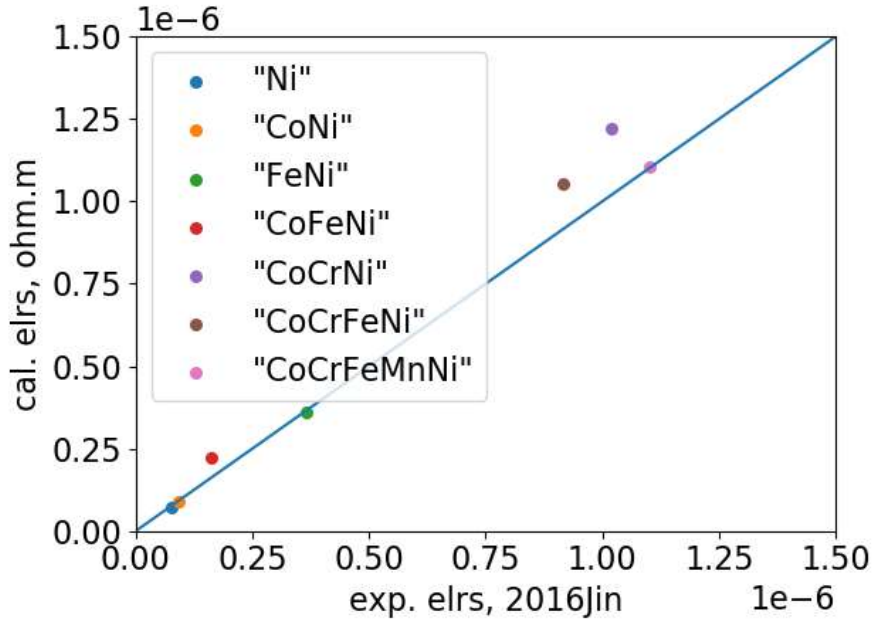

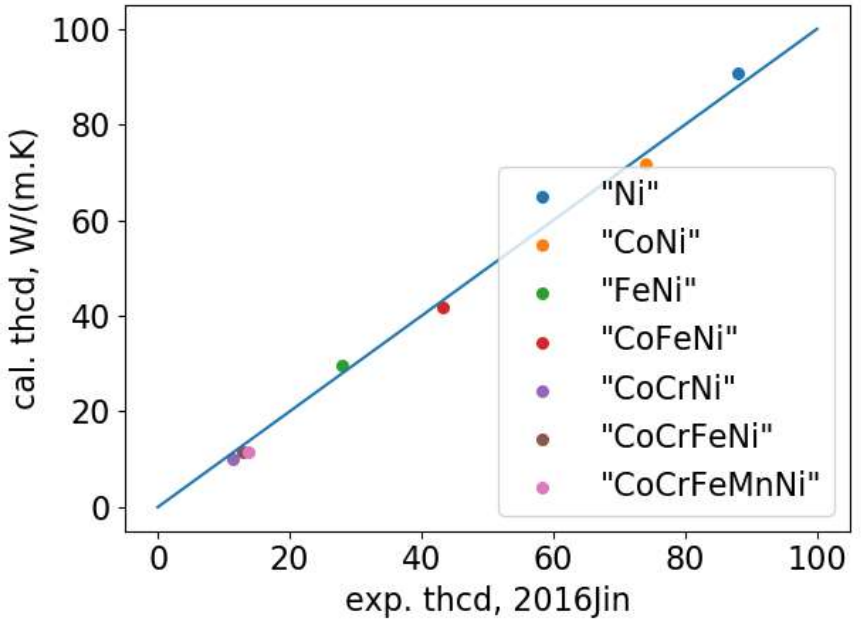

Jin et. al. Sci. Rep. 6(2016)20159

Viscosity

Case study: Fe-Cr-Ni

- Binary systems:

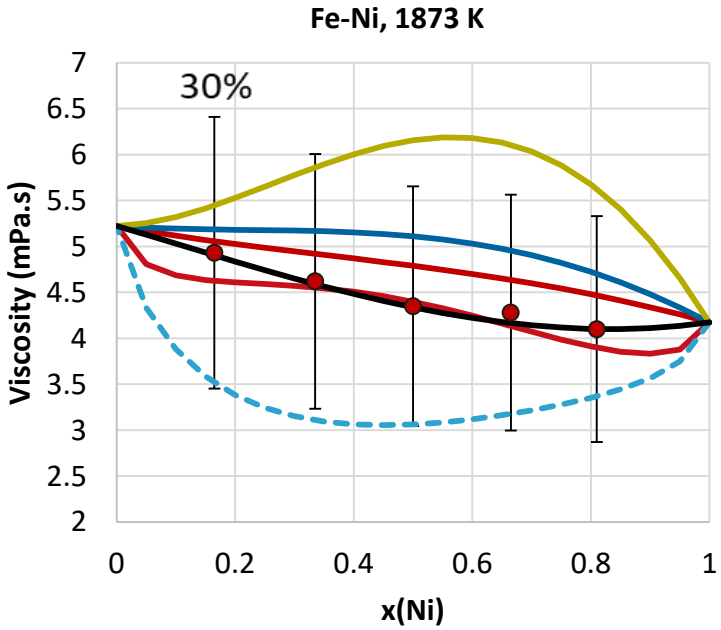

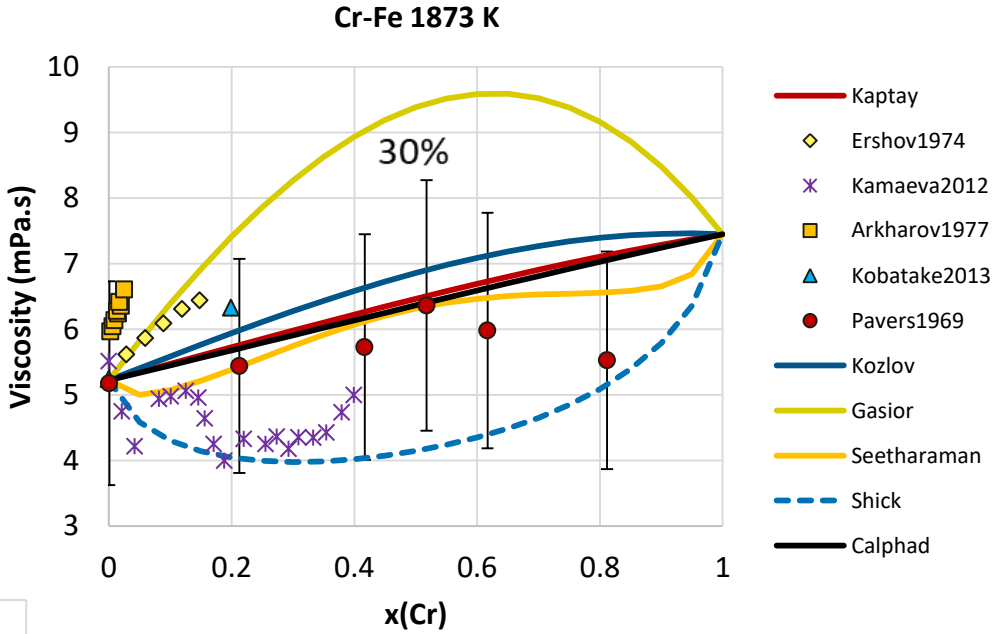

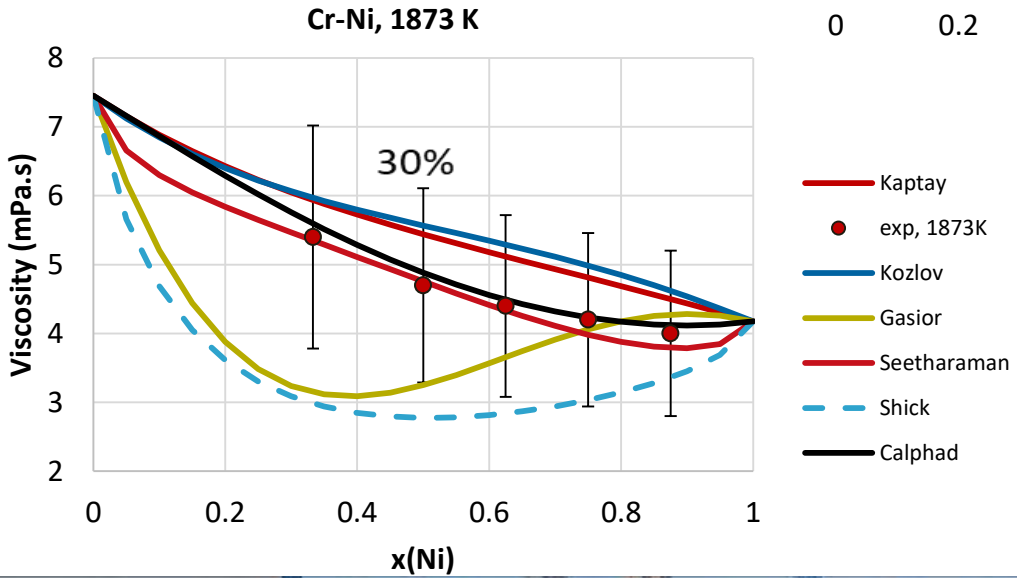

Case study: Fe-Cr-Ni

- Ternary viscosities

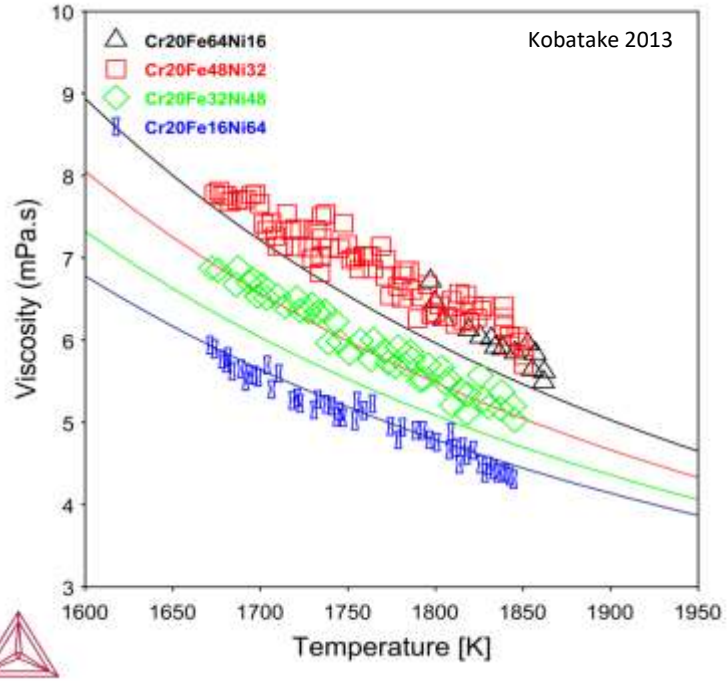

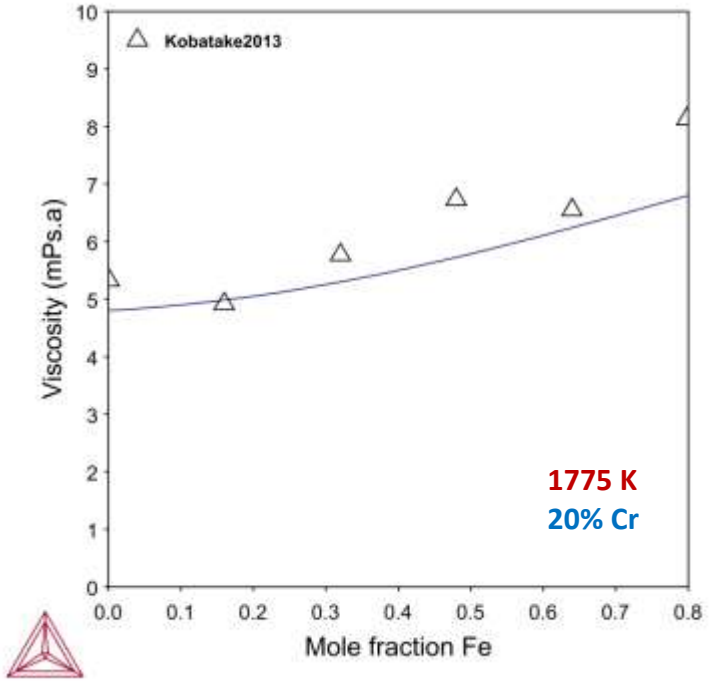

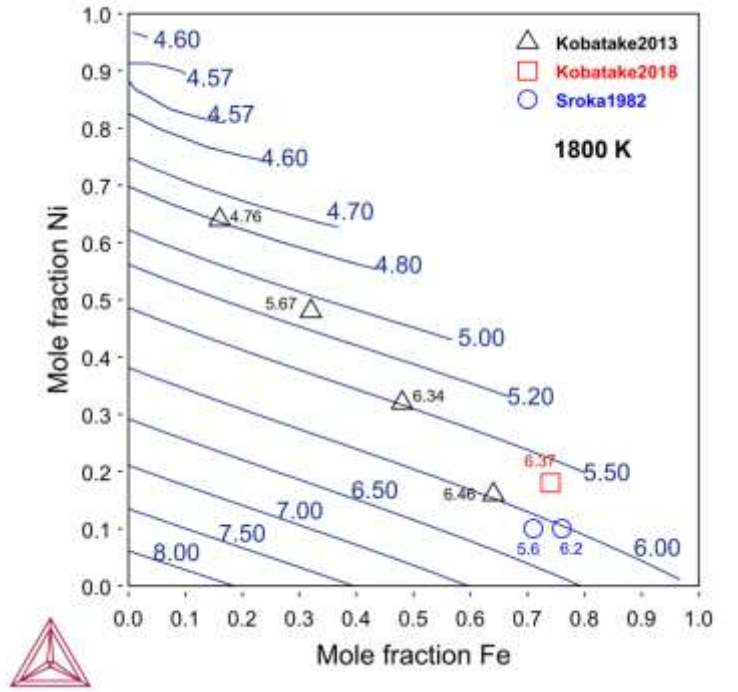

Case study: Ti-Al-Nb

Einstein-Roscoe eq:

$$\eta = \eta_0(1-c)^{-2.5}$$

where c is the volume fraction of solid and solid particles of different sizes are assumed.

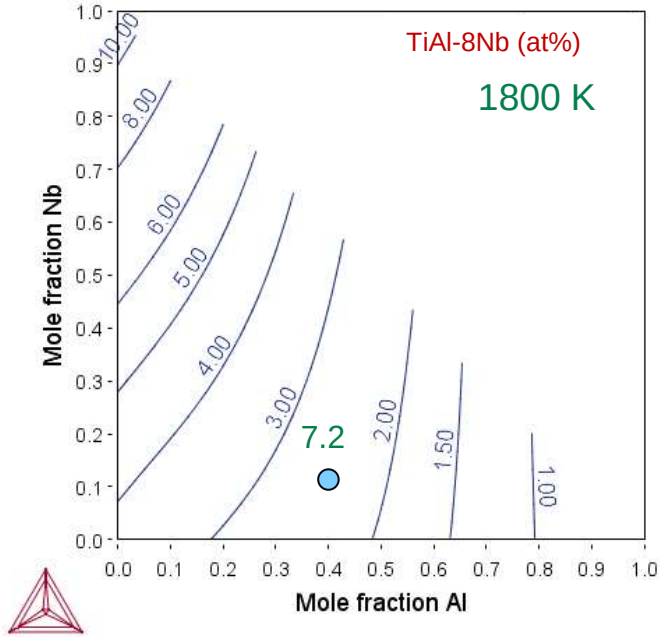

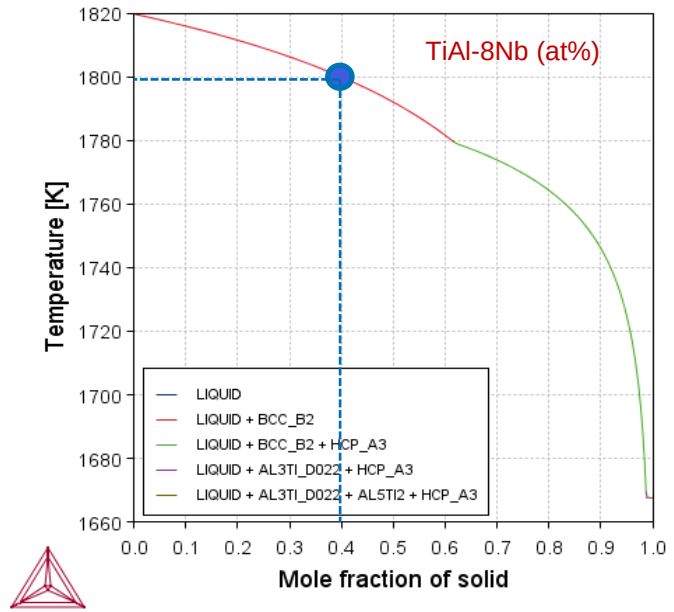

$$\eta = 2.18(1-0.4)^{-2.5} = \mathbf{7.8}\ \text{mPa.s}$$

Exp data from: Wunderlich et al, Adv. Eng. Mater. (2018) 1800346

Average deviations by each model predicting viscosities of $CaO\text{-}MgO\text{-}Al_2O_3\text{-}SiO_2$ system *

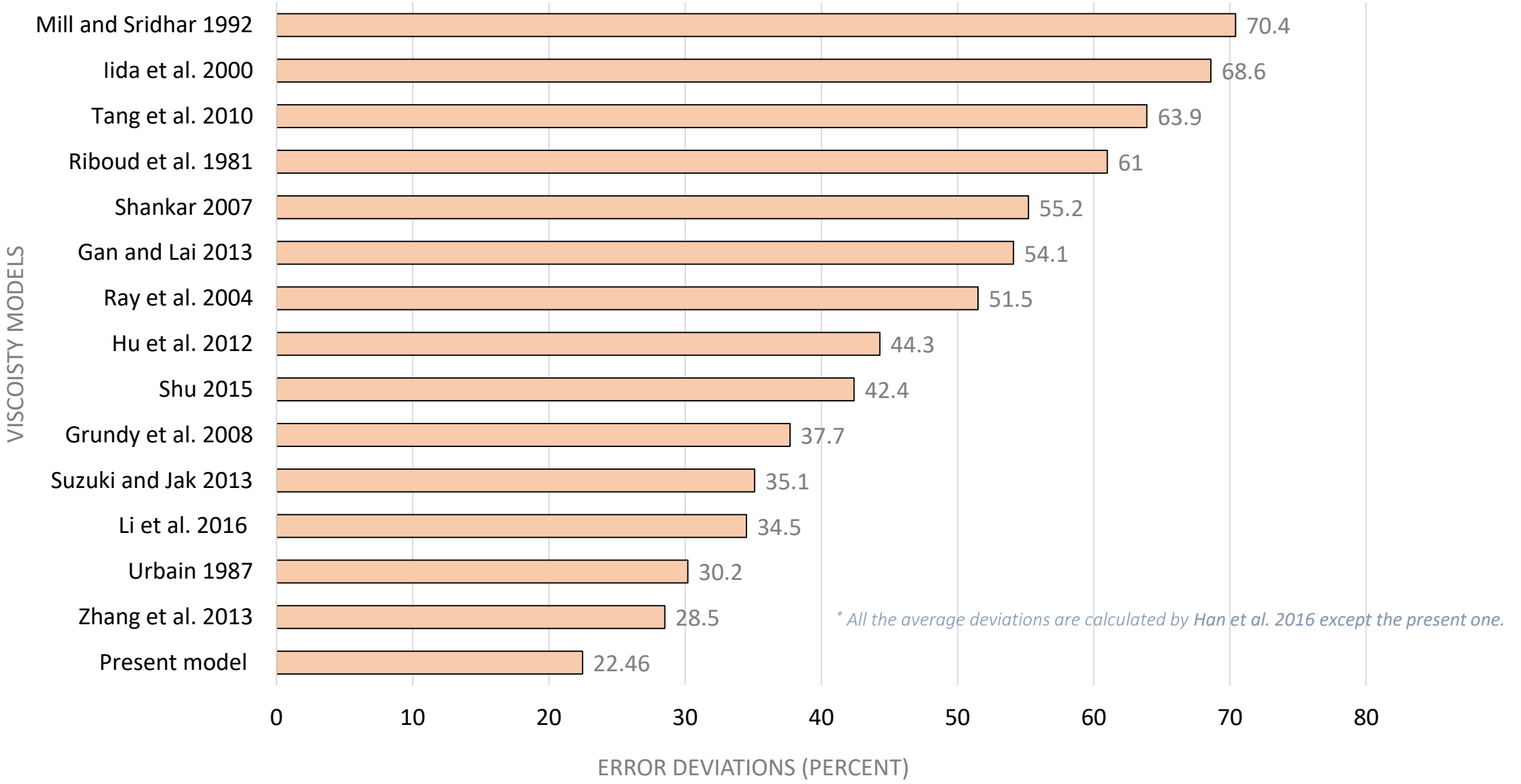

** All the average deviations are calculated by Han et al. 2016 except the present one.*

Summary and Ongoing Work

Databases on

Thermal conductivity/resistivity

Electric conductivity/resistivity

Viscosity

Surfact tension

Congratulations!